DESY 07-135
September 2007

Prospects of a Search for a New Massless Neutral Gauge Boson at the ILC

E. Boos[1], V. Bunichev[1] and H.J. Schreiber[2]

[1] Skobeltsyn Institute of Nuclear Physics, MSU, 119992 Moscow, Russia

[2] DESY, Deutsches Elektronen-Synchrotron, D-15738 Zeuthen, Germany

Abstract

Prospects to search for a new massless neutral gauge boson, the paraphoton, in e^+e^- collisions at center-of-mass energies of 0.5 and 1 TeV are studied. The paraphoton naturally appears in models with abelian kinetic mixing. A possible realistic model independent lowest order effective Lagrangian contains magnetic interactions of the paraphoton with the Standard Model fermion fields. These interactions are proportional to the fermion mass and grow with energy, with however very weak paraphoton couplings to ordinary matter. At the ILC, a potentially interesting process to search for the paraphoton is its radiation off top quarks, so that the event topology to be searched for is a pair of acoplanar top quark jets with missing energy. By combining many discriminating features of signal and background events efficient paraphoton event selection was achieved allowing to set limits for the top-paraphoton coupling. Arguments in favor of the missing energy as the paraphoton with spin 1 are discussed.

1 Introduction

Modern elementary particle field theories are based on principe of the gauge invariance. It means that the Lagrangian of the theory should be invariant with respect to group transformation of the local symmetry which leads to a corresponding number of massless vector gauge boson fields. In the Standard Model (SM), based on the $U_Y(1)\times SU_L(2)\times SU_C(3)$ gauge symmetry group, 12 gauge vector bosons exist. Three of them, the electroweak bosons $W^{\pm}$ and Z^0, get masses due to the Higgs mechanism of spontaneous symmetry breaking. The eight massless strongly interacting gauge bosons, the gluons, are confined in hadrons and only one directly observed massless neutral vector boson, the well known photon, exists within the SM.

Although the Standard Model does not require any additional gauge fields it is possible to introduce gauge invariant operators in the Lagrangian which involve new gauge fields not forbidden by basic principe of gauge invariance. An example is given in [1] by the abelian kinetic mixing of the SM $U_Y(1)$ field with a new $U_P(1)$ field in a gauge invariant manner. The mixing term of the two $U(1)$ fields can be diagonalized and canonically normalized by an $SL(2,R)$ transformation in a way that one linear combination of the fields corresponds to the ordinary photon which couples in the usual manner to all electrically charged particles within the SM. The other linear combination appears as a massless spin-1 neutral particle, referred to as the 'paraphoton' in [2] and denoted by γ' in this paper. This mechanism also provides an elegant way of introducing millicharged particles[1] into the theory [3]. The paraphoton couples directly to millicharged fermions and only indirectly to the SM fields via higher mass-dimension operators.

In this study we follow an approach proposed in [4] where the effective Lagrangian of the interaction of the paraphoton with the SM fermion fields was proposed by considering higher dimensional operators. A possible lowest order Lagrangian which preserves both the new $U_P(1)$ and the SM gauge symmetries with the SM fermion cirality structure has the following form:

$$\frac{1}{M^2}P_{\mu\nu}\left(\bar{q}_L\sigma^{\mu\nu}C_u\tilde{H}u_R+\bar{q}_L\sigma^{\mu\nu}C_dHd_R+\bar{l}_L\sigma^{\mu\nu}C_eHe_R+h.c\right), \tag{1}$$

where q_L, l_L are the quark and lepton doublets, u_R, d_R the up and down-type $SU(2)$ singlet quarks, e_R the electrically-charged $SU(2)$-singlet leptons, and H is the Higgs doublet. An index labeling the three fermions generations is implicit here. The 3×3 matrices in flavor space, C_u, C_d, C_e, have dimensionless complex elements, and M is the mass scale where the operators are generated.

[1] Millicharged particles are related to fields charged under the $U_P(1)$ group. Interaction of these particles with SM fields should be very small and proportional to the kinetic mixing parameter.

One can see that the interactions of the paraphoton with Standard Model fermions are suppressed by two powers of the mass scale M, but are directly proportional to the fermion mass m_f and the dimensionless coupling strength parameter C_f, with $f = u, d, e$. The coefficients C_f are unknown, but various phenomenological constraints exist. In particular, limits on these parameters for light fermions were, for example, deduced from paraphoton annihilation to muon pairs, $\gamma'\gamma \to \mu^+\mu^-$, or the Compton-like process, $\gamma'\mu^\pm \to \gamma\mu^\pm$, assuming the γ' interaction rate equals the expansion rate of the universe at freeze out. Together with successful predictions of primordial nucleon-synthesis the $\mu^-\mu^+\gamma'$ coupling parameter is bounded to $M/\sqrt{c_\mu} \gtrsim 1.5$ TeV, where c_μ is related to C_μ via $c_f = C_f v_h/(\sqrt{2}m_f)$, with v_h the vacuum expectation value of the Higgs field. Or, star cooling by γ' emission constraints the electron-paraphoton interaction since the associated energy loss is proportional to the square of $4c_e{m_e}^2/M^2$. The limit on γ' emission through Bremsstrahlung, such as $e^- + {}^4He \to e^- + {}^4He + \gamma'$, from the core of red giant stars [7] requires $M/\sqrt{c_e} \gtrsim 3.2$ TeV, while Compton-like scattering, $\gamma e^- \to \gamma' e^-$, in horizontal-branch stars sets a somewhat weaker limit of $M/\sqrt{c_e} \gtrsim 1.8$ TeV. A constraint on the γ'-coupling to nucleons of $M/\sqrt{c_N} \gtrsim 7$ TeV has been estimated from the neutrino signal of the supernova 1987A assuming the supernova was cooled predominantly by neutrinos. More details of possible lower limits on γ' interactions with fermions are discussed in [4].

An intriguing aspect of the presence of an additional gauge field like the paraphoton is the possible existence of fields charged under the $U_P(1)$ group. Simple renormalizable models generate operators, see eq.(1), which are associated with new heavy states. The lightest particle of this type with negligible electrical charge is stable and could be a viable dark matter candidate.

To summarize, a massless neutral gauge boson other than the SM photon may exist. It interacts with ordinary matter via higher-order operators. The rather weak bounds on the mass scale M makes it worthwhile to search for this new photon-like state in future collider experiments. From the Lagrangian, eq.(1), follows that due to the proportionality of the γ' couplings to the fermion mass, γ' interaction with SM particles is strongest with particles of the third generation, especially with the top quark, and small or negligible with light fermions. Therefore, we expect that the most interesting process to search for the paraphoton will be γ' radiation off the top quark. Since so far no constraint on c_t exists, access to $M/\sqrt{c_t}$ seems possible or corresponding limits might be set for the first time.

It seems a priori very difficult to perform γ' searches at hadron colliders because of copious $t\bar{t}$ + multi-jet background production. The next generation e^+e^- linear collider (ILC) is ideally suited to evaluate prospects of a search for the paraphoton

via the channel

$$e^+e^- \to t\ \bar{t}\ \gamma' \ . \tag{2}$$

The search strategy relies on the property of the γ' to interact weakly with ordinary matter and its favored emission from top quarks. Hence, the signal signature consists of a pair of acoplanar top quark jets with missing transverse energy, $\not{E}_T$, carried away by the paraphoton. The rate of such events if noticed should clearly exceed the expected SM background.

Simulations of $t\bar{t}\gamma'$ signal events with a 'reasonable' value of the coupling parameter $M/\sqrt{c_t}$ and SM background reactions were performed at center-of-mass energies $\sqrt{s} = 0.5$ and 1.0 TeV and an integrated luminosity of 0.5, respectively, 1 ab^{-1}. These assumptions are in accord with the present design for the ILC, initially producing collisions at 0.5 TeV and in a second stage at 1 TeV [5].

The paper is organized as follows. In section 2 basic properties of signal events are studied at the parton level in order to extract informations which might be helpful to discriminate signal from background events. Section 3 describes the search strategy for the γ' based on hadronic W decays, $W \to q\bar{q}$, to avoid complications from leptonic W decays with neutrinos in the final state, also carrying away transverse energy. The analysis is performed based on full simulation including ILC detector response. Section 4 discusses accessible limits on $M/\sqrt{c_t}$ from excess of signal events over the SM background expectations and arguments in favor of the nature of the paraphoton are presented. Conclusions are summarized in section 5.

2 The signal reaction $e^+e^- \to t\ \bar{t}\ \gamma'$

The characteristics of the signal reaction $e^+e^- \to t\ \bar{t}\ \gamma'$ were computed and corresponding partonic events were generated by means of the program package CompHEP [8]. The Feynman rules for the fermion-fermion-γ' vertices following from the effective Lagrangian (1)

$$\frac{c_f}{M^2} \cdot m_f \cdot p_\nu^{\gamma'} \left(\gamma^\nu \gamma^\mu - \gamma^\mu \gamma^\nu\right) \tag{3}$$

have been implemented into CompHEP allowing variations of the free coupling parameter $M/\sqrt{c_t}$. An interface with PYTHIA 6.202 [9] simulates initial and final state radiation and jet hadronization, needed at a later stage of our study. Also, beamstrahlung effects [10] are taken into account.

Table 1 shows the number of signal events expected at $\sqrt{s} = 0.5$ and 1 TeV as a function of $M/\sqrt{c_t}$ for an accumulated luminosity of 0.5, respectively, 1 ab^{-1}. The

$M/\sqrt{c_t}$ $[TeV]$	$\sqrt{s} = 0.5\ TeV$	$\sqrt{s} = 1\ TeV$
0.2	5700	42500
0.3	1100	8500
0.5	40	1100
1	10	70

Table 1: $t\bar{t}\gamma'$ event rates for several values of $M/\sqrt{c_t}$ at $\sqrt{s} = 0.5$ and 1 TeV and an integrated luminosity of 0.5, respectively, 1 ab^{-1}.

event rates become rapidly smaller with increasing $M/\sqrt{c_t}$, so that in particular for large $M/\sqrt{c_t}$ values γ' detection is challenging. Simulations were only performed for $M/\sqrt{c_t} = 0.2$ TeV enabling sufficient γ' events at both energies. It is worth to mention that below $M/\sqrt{c_t} \simeq 0.1$ TeV the kinetic mixing parameter of the $U_Y(1)$ and $U_P(1)$ becomes relatively large and leads to millicharged particles with electric charges larger than 10^{-4}. Such particles should have been detected in various SM reactions, contrary to experimental findings. One should also point out that the effective interaction Lagrangian approach cannot be applied for $M/\sqrt{c_t} \lesssim 0.1$ TeV since the effective coupling parameter $\frac{c_t m_{top} E}{M^2}$ gets to large for typical collision energies E.

In order to establish a search strategy for the paraphoton in $t\bar{t}$ events it is advantageous to know whether an off-shell or on-shell top quark radiates the γ'. Fig. 1 shows the invariant mass of the $\gamma' Wb$ system of that top which radiates the paraphoton. Besides of a tiny fraction of events with a $\gamma' Wb$ invariant mass at the top mass, most of the events have a $\gamma' Wb$ mass larger than m_{top}. These events have the corresponding Wb invariant mass close to the top mass. Therefore, the paraphoton is radiated off a top being off-shell in most cases, and γ' search strategies should rely on an on-shell top with $t \to Wb$ decay in association with the γ'. Since the signature of the γ' relies on negligible interaction strength with ordinary matter, its transverse momentum and energy behavior is essential for its finding. Fig. 2 shows both variables at 1 TeV. Note that substantial transverse momentum, respectively, energy is carried away by the γ', so that large missing transverse momentum, $\not{p}_T$, and/or missing energy, $\not{E}$, will tag signal events.

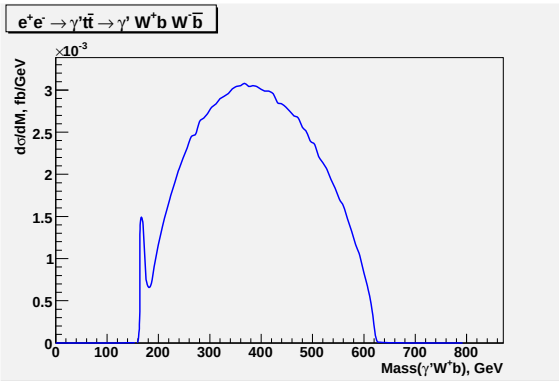

Figure 1: Invariant mass of the $\gamma' Wb$ system.

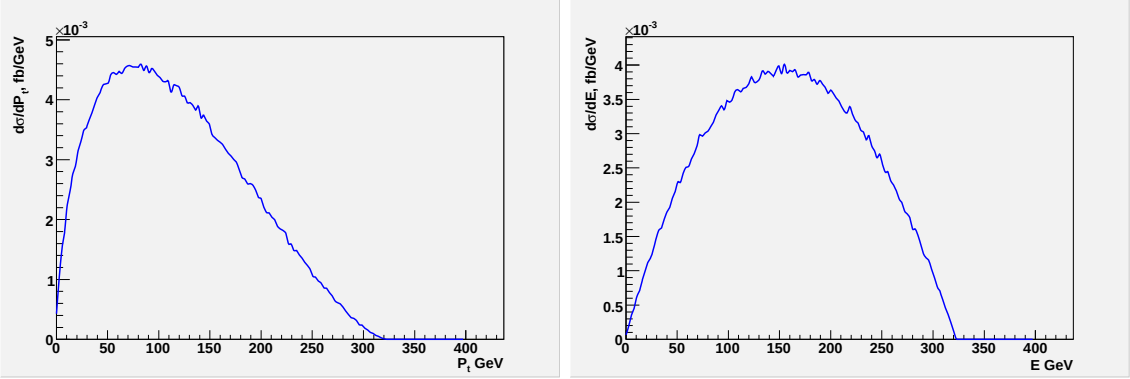

Figure 2: γ' transverse momentum (left) and energy (right) distributions at $\sqrt{s} = 1$ TeV.

3 Signal event selection

After event generation using CompHEP, PYTHIA and the CompHEP-PYTHIA interface with the Les Houches Accord implemented [12], an approximate response of an ILC detector was simulated with the package SIMDET_v4 [13] resulting to 'measured' tracks and energy clusters in the calorimeters. Including a simple particle flow algorithm, the output of SIMDET denoted as 'energy flow objects' was subject to our search studies.

Basic properties of the signal process as discussed in the previous section may suggest that a reasonable separation of $t\bar{t}\gamma'$ events from large SM background should be possible. However, there are a number of SM background sources which have

$background$	$\sqrt{s} = 0.5\ TeV$	$\sqrt{s} = 1\ TeV$
$t\bar{t}(\gamma)$	276675	200310
$t\bar{t}\nu\bar{\nu}$	75	930

Table 2: Background events at $\sqrt{s} = 0.5$ and 1 TeV for an integrated luminosity of 0.5, respectively, 1 ab^{-1}.

similar or identical final state signatures, i.e. a signature of $t\bar{t} + \not{E}_T$ with acoplanar top quark jets. The most important background consists of $t\bar{t} + (\gamma)$ events, where the γ from initial state radiation (ISR) is very often not detected. The number of events expected for both energies are given in Table 2. They exceed substantially the number of signal events for interesting $M/\sqrt{c_t}$ values. Fig. 3 shows the photon energy for such events without cuts and with the demand $cos(\theta_\gamma) > 0.95$ in comparison to the γ' distribution from signal events.As can be seen, the paraphoton energy spectrum

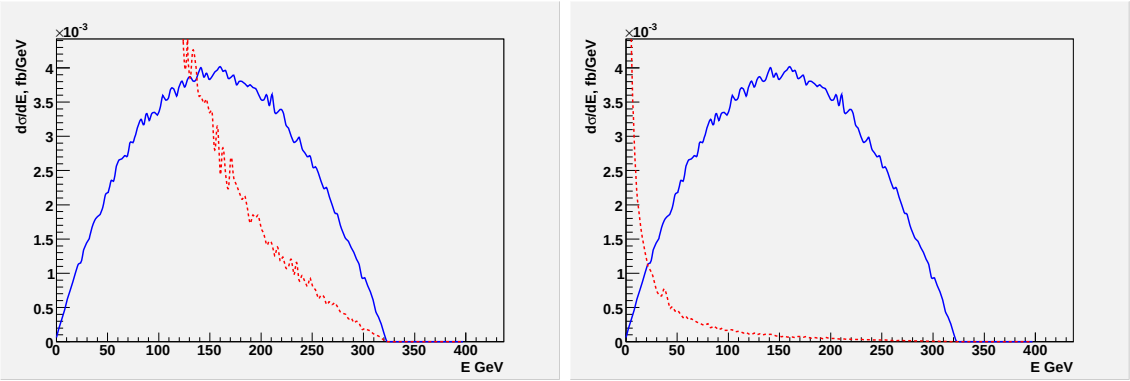

Figure 3: Energy spectrum of the γ (dotted line) from $t\bar{t} + (\gamma)$ background and the γ' (solid line) from $t\bar{t}\gamma'$ signal events. The left side shows the spectra without any cut, the right one with the cut $cos(\theta_\gamma) > 0.95$.

is very different from the background photon spectrum. The γ' energy rises due to the momentum proportionality of its coupling with the top quark. In contrast, the ISR photon spectrum peaks at zero, which makes the photon energy a potentially sensitive dicsriminating variable. Obviously, a veto on registered photons with small polar angle would discard a substantial fraction of this background. However, in practice photons with very low θ_γ are not accessible and copious small polar angle π^0 and γ production from quark fragmentation occurs, and a veto on final state photons would also eliminate signal events. Hence, such a cut will not be applied in

this study.

The next significant background to consider is the channel $e^+e^- \to t\bar{t} + \nu\bar{\nu}$, with a signature similar to that of the signal due to escaping neutrinos in the final state, with $\nu\bar{\nu}$ pairs coming mostly from Z decays. The corresponding event numbers also given in Table 2 are comparable to the signal event rates for not too small $M/\sqrt{c_t}$ values, but orders of magnitude smaller than the dominant $t\bar{t}(\gamma)$ background. An invariant mass cut of e.g. $M_{\nu\bar{\nu}} < 80$ GeV, i.e. a cut on the event missing mass, removes most of the $t\bar{t} + \nu\bar{\nu}$ events.

Additional SM background with a topology of a pair of acoplanar top quark jets and large $\not{E}_T$ is not needed to be addressed. It will be difficult for any SM event to mimic the topology of interest, so that the only source of potential background to consider consists of $e^+e^- \to t\ \bar{t}\ (\gamma)$ events. It is important to have some good understanding of this reaction in order to establish an excess of paraphoton candidate events over the background.

In a first attempt, a conventional method was applied by using consecutive cuts on kinematical variables based on either the energy flow objects or, utilizing a jet finder, the 4-momenta of jets consistent with the $t\bar{t} \to (Wb)(Wb) \to (q\bar{q})b\ (q\bar{q})b$ decay chain. The variables used may be classified into three categories: global event kinematics, variables based on jet properties and variables based on jet correlations. We considered the missing event energy, $\not{E}$, missing transverse energy, $\not{E}_T$, missing momentum, $\not{p}$, missing transverse momentum, $\not{p}_T$, the event aplanarity, thrust, missing mass squared, the angle between the top momenta and the coplanarity angle (the angle between the beam, the t and $\bar{t}$) as well as, for a given hemisphere, the largest energy of jets and the largest angle between two jets. Jets were reconstructed by means of the routine PUCLUS from PYTHIA which relies on a cluster analysis method using particle momenta. The 'jet-resolution-power' was adjusted to provide 7- and 8-jet event rates in accord with expectations from gluon radiation. The method of consecutive cuts, however, was found to be inefficient to select signal from background because of the failure of distinct properties between signal and background events.

In cases of large background, small signal event rates and of variables with only small discrimination power one needs to pursue more sophisticated strategies to extract the signal. Out of several powerful multivariate selection methods we used the following. Kinematical variables as discussed above were combined into a global discriminant variable P_P, designed to give a measure of the 'Paraphoton-likeness' of any particular event. This quantity was constructed from the variables after normalization based on large statistics samples of simulated signal and background events. For each event and variable i, signal and background probabilities (P_S^i,

respectively, P_B^i) were then calculated, and by multiplication of all signal probabilities ($\prod_{i=1}^{n} \frac{P_S^i}{P_S^i+P_B^i}$, i=1 ... n, with n=18, the number of variables taken into account) the sensitivity for an event to be a paraphoton candidate was maximized. The quantity so obtained was constraint to lie in the region [0;1]. Background events are preferentially distributed at low P_P values while for signal events P_P is close to unity. The distributions of P_P for both center-of-mass energies considered are shown in Fig. 4. Clear accumulations of γ' candidate events can be recognized near $P_P = 1$, with some non-negligible background in particular at 0.5 TeV. A cut of $P_P > 0.98$ was applied to select signal events. This method resulted in a γ' selection efficiency of 49% (76%) at $\sqrt{s} = 0.5$ (1) TeV, while only 9% of background events at both energies survived. The 'Paraphoton-likeness' technique results to significantly better signal-to-background ratio than the method using consecutive cuts. Therefore, we rely on the results of this method and demand $P_P > 0.98$ as the principal cut in the study.

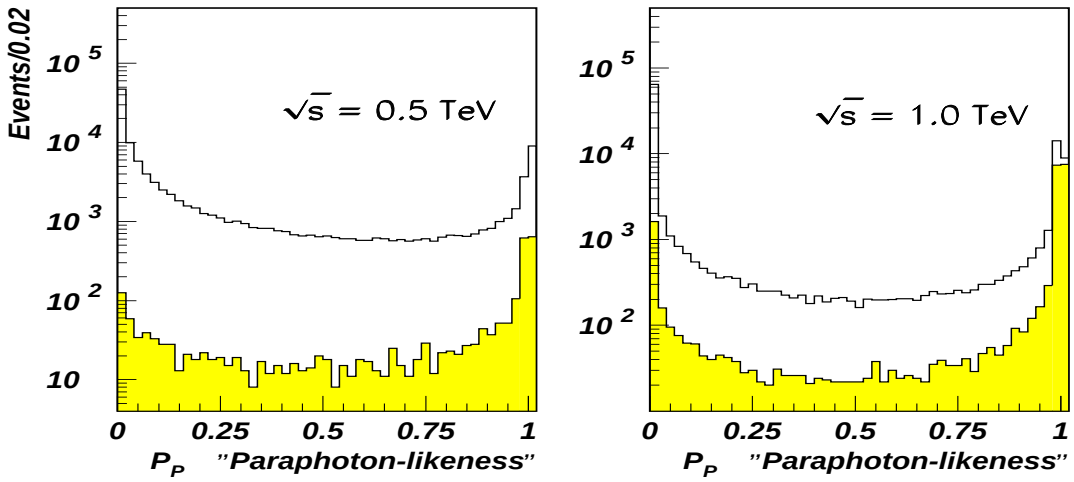

Figure 4: Distributions of the discriminant variable P_P for $t\bar{t}\gamma'$ signal events (shaded) and the sum of signal and background events at $\sqrt{s} = 0.5$ (left) and 1 TeV (right).

At $\sqrt{s} = 0.5$ TeV after application of the likeness cut, $S/\sqrt{B}$ results to 11.96 for $M/\sqrt{c_t} = 0.2$ TeV, while $S/\sqrt{B}$ is 162.6 at 1 TeV, i.e. the chance of measuring the signal event rates as a result of a background fluctuation is $0.5 \cdot 10^{-12}$ and $< 10^{-15}$ at 0.5, respectively, 1 TeV, using Gaussian sampling of uncertainties. These numbers clearly demonstrate that background fluctuation cannot be responsible for the excess.

Including a conservative 3% uncertainty of the $t\bar{t}(\gamma)$ background rate would not alter the conclusions on the highly significant excess of γ' events.

Fig. 5 shows the $\not{E}_T$ and $\not{p}_T$ distributions at 0.5 and 1 TeV for the signal events (shaded) and the sum of signal and background events, surviving the cut $P_P > 0.98$. As apparent from Fig. 5, convincing excess of paraphoton events is evident in both distributions at 1 TeV and the ratio $S/\sqrt{B}$ being in the order of 162 can be further enhanced by demanding, for example, $\not{E}_T > 330$ GeV or $\not{p}_T > 100$ GeV. In this way, an almost background-free signal event sample can be extracted for further measurements. The situation is much less convenient at 0.5 TeV, where reasonable signal event extraction with small background is difficult to achieve. Improvements are, however, expected for $M/\sqrt{c_t}$ 'coupling' values less than 0.2 TeV (see Table 1) so that γ' physics can also be probed during the first phase of the ILC.

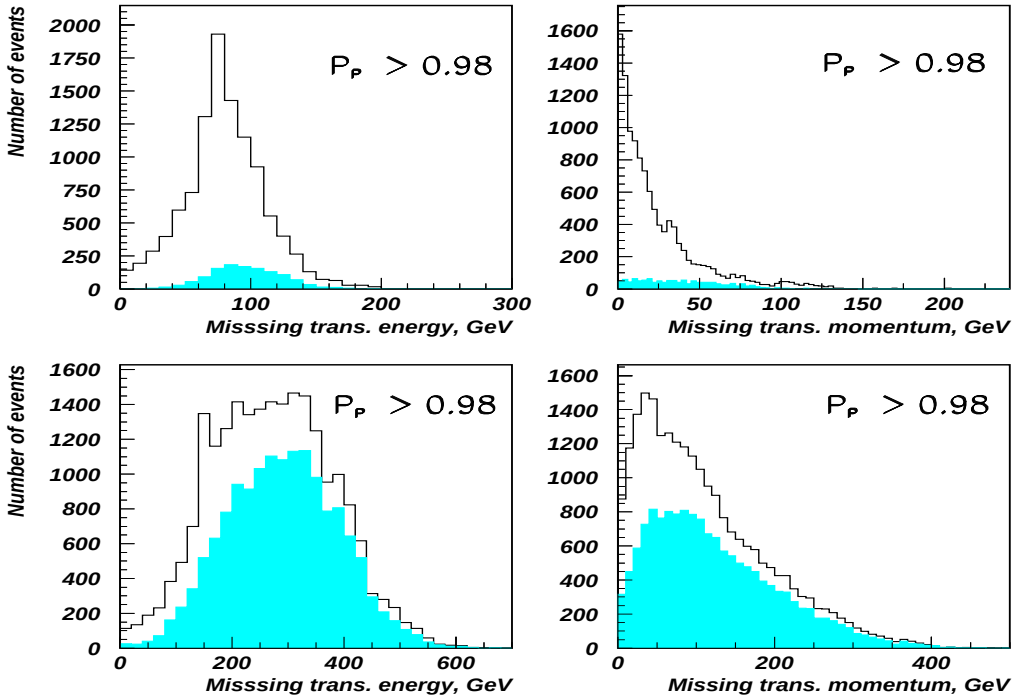

Figure 5: $\not{E}_T$ and $\not{p}_T$ distributions of $t\bar{t}\gamma'$ signal events (shaded) and the sum of signal and background events at $\sqrt{s} = 0.5$ (top) and 1 TeV (bottom).

4 Discussion of the results

If an excess of signal events over SM background expectations has been established, limits on $M/\sqrt{c_t}$ accessible for a significance[2] of $S/\sqrt{B} = 5$ can be derived. We consider this figure as sufficient for discovery the paraphoton characterized by acoplanar top quark jets with large $\not{E}_T$, carried away by the γ'. The number of surviving γ' events for 5σ discovery amounts to 508 (450) at 0.5 (1) TeV for an integrated luminosity of 0.5 (1.0) ab^{-1}. These numbers can be converted into a limit for the 'coupling' parameter $M/\sqrt{c_t}$ of 0.33 (0.61) TeV, with the 1 TeV value of 0.61 TeV as the most stringent limit accessible at the ILC.

We will also discuss the signal-to-background ratio, S/B, as it will be important for attempting to understand the nature of the excess events. For that, we would like to have a clean sample of events that we understand to be mostly signal. This is especially important for studying variables in favor of the interpretation of the missing energy as the paraphoton. Large numbers of background events would dilute signal properties and hence complicate correct interpretations. At $\sqrt{s} = 0.5$ TeV, the small S/B ratio of 0.11 does not favor such an analysis despite of small possible improvements of the performance by additional cuts. At 1 TeV, however, the ratio S/B of 1.79 is sufficiently large so that background contamination should not be a major worry. If we require in addition $\not{E}_T >$ 330 GeV, the number of signal to background events results to $5231/2654 = 1.97$.

In order to demonstrate the spin-1 nature of the γ', we follow studies performed to establish the vector nature of the gluon in 3-jet e^+e^- annihilation events at PETRA [14–17] and LEP [18–20] energies, based on predictions that a spin-$\frac{1}{2}$ quark radiates the spin-1 gluon. Many observables have been measured, including the Ellis-Karlinger angular distribution [21], energy-energy correlations [22], jet masses [23] as well as the three-jet [24] and multi-jet production cross sections [25], all of which were important in establishing the properties of the gluon, in particular its spin.

For the sake of demonstration, we assign for each 1 TeV signal event candidate with $\not{E}_T >$ 330 GeV, the fracional energy variables $x_i = E_i/E_b$ (i=1, 2, 3) to the t, $\bar{t}$ and γ', with E_b the nominal incident beam energy. After ordering the x_i such that $x_1 \geq x_2 \geq x_3$ and assuming the top quark mass is small with respect to E_b, a Lorentz boost is performed which brings the two less energetic jets to their c.m. frame where they should emerge back-to-back. The angle which these jets make with the thrust

[2] We will quantify the discovery potential of the γ' in the usual way of $significance = signal/\sqrt{background}$, where signal and background imply the number of corresponding events passing all cuts.

axis is defined as the Ellis-Karliner angle θ_{EK} [21]

$$cos\theta_{EK} = \frac{x_2 - x_3}{x_1} = \frac{sin\theta_2 - sin\theta_3}{sin\theta_1} \ , \tag{4}$$

where θ_i is the angle between the two jets opposite to jet i. Fig. 6 shows, after background subtraction and some detector acceptance corrections, the cosine of the Ellis-Karliner angle distribution proposed to dicriminate between the vector and scalar nature of the radiated γ', In order to avoid infrared divergences the analysis is restricted to a region safely away from $x_1 = 1$, by the cut $1 - x_1 > 0.05$. Distinction between the vector and scalar particle interpretations is made only on the basis of the shape of the distribution: a spin-1 particle provides a flat behaviour near $cos\theta_{EK}$= 0, while a spin-0 object yields a rising behaviour [14]. Thus, spin-1 assignment for the paraphoton is highly favored over spin 0.

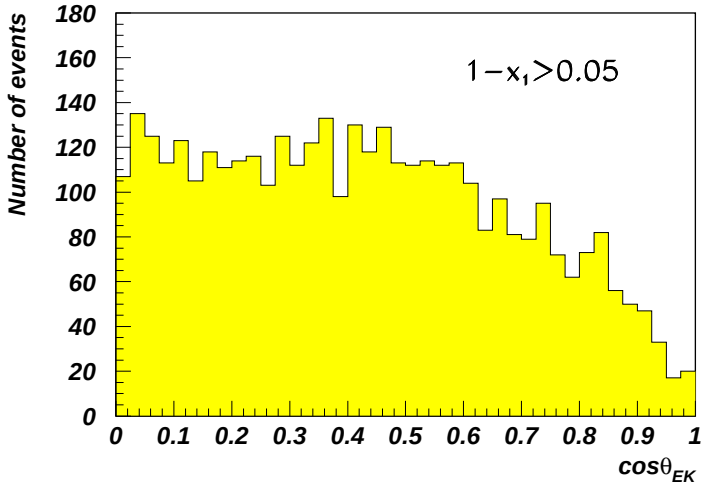

Figure 6: Cosine of the Ellis-Karliner angle θ_{EK} for 3-jet events selected at $\sqrt{s} = 1$ TeV with the additional cut $1 - x_1 > 0.05$.

Alternatively, after interpreting a signal candidate event as a 3-jet event, the polar angle distribution of the normal to the three-jet plane, θ_N, was proposed as a variable to distinguish between the vector and scalar hypothesis of the emitted particle [26,27]. We discuss shortly this variable which is defined by the cross-product of the two fastest jets as a function of a thrust cut-off T_C in order to be able to establish that the parameter α_N extrated from the distributions is (i) independent of the thrust cut-off chosen and (ii) close to $-\frac{1}{3}$ as predicted for the spin-1 interpretation of the

γ'. The cosine distributions of the angle θ_N are shown in Fig. 7 for various thrust cut-off values. The distributions, corrected for background and detector effects, were fitted to the expression

$$\frac{1}{N}\frac{dN}{dcos\theta_N} = \frac{1}{2(1+\frac{1}{3}\alpha_N)}(1+\alpha_N cos^2\theta_N) \ , \tag{5}$$

predicted for vector particle emission [28] with $\alpha_N = -\frac{1}{3}$. Good agreement between the data and the theoretical expectation is found. In particular, as seen from Table

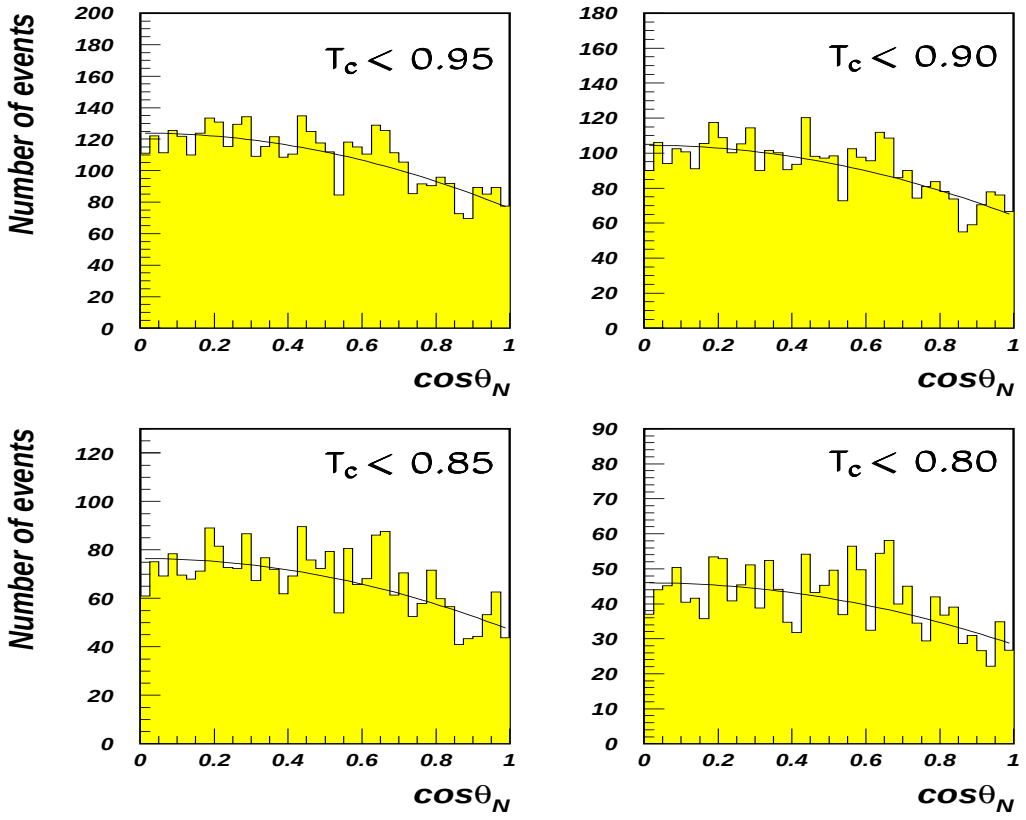

Figure 7: Polar angle distributions of the normal to the three-jet plane for four different thrust cut-off values at $\sqrt{s} = 1$ TeV. The curves represent the results of the fits described in the text.

3, the α_N values are found to be independent of the thrust cut-off and quite close to

$-\frac{1}{3}$, despite of neglecting detailed correction factors in the analysis.

T_C	α_N
0.95	-0.386 ± 0.036
0.90	-0.382 ± 0.039
0.85	-0.385 ± 0.045
0.80	-0.384 ± 0.058
0.75	-0.411 ± 0.072

Table 3: Values of the parameter α_N for the normal to the three-jet plane with $T < T_C$ at $\sqrt{s} = 1$ TeV.

5 Conclusions

Some realistic extensions of the Standard Model of elementary particle physics suggest the existence of a new massless neutral gauge boson, denoted as the paraphoton γ' in this study. This particle is similar to the ordinary photon, but the couplings of the γ' are very distinct: interactions with SM fermions are negligible except those with the top quark. Hence, if the paraphoton is radiated off the top the signature of γ' events in the channel $e^+e^- \to t\,\bar{t}\,\gamma'$ consists of a pair of acoplanar top quark jets with missing transverse energy, $\not{E}_T$, carried away by the paraphoton. Only the all-hadronic top decay mode was selected to ensure a high signal-to-background ratio and to avoid complications due to final state neutrinos in leptonic W decays.

Based on a multivariate search strategy prospects to discover the γ' at the ILC are studied. This method was necessary to pursue because large $t\bar{t}(\gamma)$ SM background, small signal event rates and little discrimination power of variables restricted an effective signal selection by the method of consecutive cuts. Maximizing the probability of each event to be a paraphoton candidate, 49% (76%) of the signal (S) at 0.5 (1) TeV was selected and the background (B) strongly suppressed, resulting to a $S/\sqrt{B}$ larger than 150 at $\sqrt{s} = 1$ TeV. Allowing for a 5σ γ' discovery significance, limits on the paraphoton-top quark 'coupling' $M/\sqrt{c_t}$ were derived. Assuming that the SM provides the only source of background, e^+e^- collisions at 1 TeV will bound this parameter to $M/\sqrt{c_t} \lesssim 0.61$ TeV, which seems to be the most stringent limit accessible at the next generation colliders since huge background expected at the LHC would prevent an improved number.

For the sake of demonstration and simplicity two angular variables, the Ellis-Karliner angle and the polar angle of the normal to the $t\,\bar{t}\,\gamma'$ plane as a function of

a thrust cut-off, were studied to establish the vector nature of the γ'. After the cut $\not{E}_T > 330$ GeV to improve the purity of the signal sample and $1 - x_1 > 0.05$ for the cosine of the Ellis-Karliner angular distribution, with x_1 the fractional energy of the fastest parton, both angular distributions are in accord with the spin-1 assignment of the paraphoton and inconsistent with e.g. a scalar hypothesis.

Acknowledgment

The work of E.B. and V.B. is partly supported by the grant NS.1685.2003.2 of the Russian Ministry of Education and Science. V.B. also acknowledges support of grant of the "Dynasty" Foundation. E.B. and V.B. are grateful to DESY and Fermilab for the kind hospitality. We thank Bogdan Dobrescu for valuable discussion and reading of the manuscript.

References

[1] B. Holdom, Phys. Lett. **B166** 196 (1986) and Phys. Lett. **B178** 65 (1986).

[2] L. B. Okun, Sov. Phys. JETP **56** 502 (1982), [Zh. Eksp. Teor. Fiz. **83** 8921 (1982);
L. B. Okun, M. B. Voloshin and V. I. Zakharov, Phys. Lett. **B138** 115 (1984);
A. Y. Ignatiev, V. A. Kuzmin and M. E. Shaposhnikov, Phys. Lett. **B84** 315 (1979).

[3] H. Goldberg and L. J. Hall, Phys. Lett. **B174** 151 (1986);
M. I. Dobroliubov and A. Y. Ignatiev, Phys. Rev. Lett. **65** 679 (1990);
R. N. Mohapatra and I. Z. Rothstein, Phys. Lett. **B247** 593 (1990).

[4] B. A. Dobrescu, Phys. Rev. Lett. **94**, 151802 (2005), arXiv:hep-ph/0411004.

[5] The ILC reference design report (RDR) is available from *http://www.linearcollider.org/cms/.*

[6] S. Hoffmann, Phys. Lett. **B193**, 117 (1987).

[7] M. Pospelov and A. Ritz, Phys. Rev. **D63**, 073015 (2001), arXiv:hep-ph/0010037.

[8] A. Pukhov et al., Report INP-MSU 98-41/542, arXiv:hep-ph/9908288;
E. Boos et al., Nucl. Instrum. Meth. **A534**, 250 (2004), arXiv:hep-ph/0403113.

[9] T. Sjostrand, L. Lonnblad, S. Mrenna and P. Skands, *PYTHIA 6.3: Physics and manual*, arXiv:hep-ph/0308153.

[10] J. A. Aguilar-Saavedra et al., *TESLA Technical Design Report Part III: Physics at an e^+e^- Linear Collider*, arXiv:hep-ph/0106315.

[11] A. S. Belyaev et al., *CompHEP-PYTHIA interface: Integrated package for the collision event generation based on exact matrix elements*, arXiv:hep-ph/0101232.

[12] E. Boos et al., *Generic user process interface for event generators*, arXiv:hep-ph/0109068.

[13] M. Pohl and H. J. Schreiber, *SIMDET - Version 4: A parametric Monte Carlo for a TESLA Detector*, arXiv:hep-ex/0206009.

[14] R. Brandelik et al., Phys. Lett. **B97** 453 (1980): S. Wu, Phys. Rep. **107** 162 (1984).

[15] H.J. Behrend et al., Phys. Lett. **B110** 329 (1982).

[16] Ch. Berger et al., Phys. Lett. **B97** 459 (1980).

[17] D. Burger et al., *Proceedings of the 21^{st} Internationale Conference on High Energy Physics*, Paris 1982, J. Phys. (Paris) **43**, C3-C6.

[18] G. Alexander et al., Z. Phys. **C52** 543 (1991).

[19] B. Adeva et al., Phys. Lett. **B263** 551 (1991).

[20] P. Abreu et al., Phys. Lett. **B274** 498 (1992).

[21] J. Ellis and I. Karliner, Nucl. Phys. **B148** 141 (1997).

[22] W. Braunschweig et al., Z. Phys. **C36** 349 (1987).

[23] J.del Peso, Ph.D. Thesis, Universad Autonoma de Madrid, FTUAM-EP-89-02, unpublished.

[24] M. Althoff et al., Z. Phys. **C29** 29 (1985).

[25] W. Braunschweig et al., Phys. Lett. **B214** 216 (1988).

[26] G. Kramer, G.Schierholz and J. Willrodt, Phys. Lett. **B79** 249 (1978); Phys. Lett. **B80** 433 (1978) and Z. Phys. **C4** 149 (1980).

[27] K. Koller et al., Z. Phys. **C6** 131 (1980).

[28] J. Koerner, G.A. Schuler and F. Barreiro, Phys. Lett **B188** 272 (1987).